HYDROLOGICAL PROCESSES
Hydrol. Process. **19**, 115–135 (2005)
Published online in Wiley InterScience (www.interscience.wiley.com). DOI: 10.1002/hyp.5759

Geocryological processes linked to High Arctic proglacial stream suspended sediment dynamics: examples from Bylot Island, Nunavut, and Spitsbergen, Svalbard

T. D. L. Irvine-Fynn,[1]* B. J. Moorman,[1] I. C. Willis,[2] D. B. Sjogren,[1] A. J. Hodson,[3] P. N. Mumford,[3] F. S. A. Walter[1] and J. L. M. Williams[1]

[1] *Department of Geography, University of Calgary, 2500 University Drive N.W., Calgary, AB T2N 1N4, Canada*
[2] *Scott Polar Research Institute, Department of Geography, University of Cambridge, Lensfield Road, Cambridge CB2 1ER, UK*
[3] *Department of Geography, University of Sheffield, Winter Street, Sheffield S10 2TN, UK*

Abstract:

Recent research has identified differences in processes contributing to suspended sediment concentration (SSC) dynamics in proglacial streams between High Arctic and alpine catchments, but does not examine processes explicitly linked to the periglacial environment. Three glacierized basins were studied: Austre Brøggerbreen and Midre Lovénbreen, Svalbard (79 °N, 12 °E) and Glacier B28, unofficially named Stagnation Glacier, Bylot Island, Nunavut (73 °N, 78 °W). SSC variations were modelled from continuous turbidity, discharge and meteorological data throughout the summer months. Three statistical tools were utilized: principal component analysis, change-point analysis and multivariate regression. These are shown to be effective in identifying subperiods of distinctive geocryological and glaciofluvial characteristics. Multivariate regression for the subseasons included autoregressive integrated moving-average modelling, and showed that SSC variations were related not only to discharge variability, but also to fluctuations in energy fluxes. The results are interpreted in terms of spatio-temporal changes in sediment mobilization and supply associated with changes in the relative importance of fluvial, glacial and periglacial processes. This evidence supports the notion of important linkages between glacial, fluvial and periglacial systems, but exemplifies distinct variability between High Arctic glaciers. Copyright © 2005 John Wiley & Sons, Ltd.

KEY WORDS High Arctic glaciers; proglacial streams; suspended sediment concentration; principal component analysis; change-point analysis; geocryological processes

INTRODUCTION

Recent research has focused upon proglacial stream chemistry and CO_2 sequestration (e.g. Hodgkins *et al.*, 1997; Wadham *et al.*, 1998, 2001; Hodson *et al.*, 2000; Brown, 2002), modelling Arctic river sediment load (e.g. Syvitski, 2002), and environmental reconstruction from glaciolacustrine and glaciomarine records (e.g. Schiefer *et al.*, 2001). In relation to these foci, specific understanding of the controls and variability of sediment supply and delivery processes in glacierized catchments is important.

Glacier thermal regime determines whether water is present at the glacier bed and, therefore, has implications for the entrainment and release of fine sediments from glacierized catchments. Cold and polythermal glaciers, common in Arctic latitudes, often lack the extensive subglacial drainage systems common to temperate glaciers, and so Arctic glaciofluvial systems are often dominated by subaerial or ice-marginal routing rather than subglacial routing (e.g. Hodgkins, 1997; Hodson *et al.*, 1997).

In alpine temperate glacier catchments, researchers have identified a seasonal exhaustion of suspended sediment concentration (SSC) in proglacial streams, which has been interpreted in terms of the gradual

* Correspondence to: T. D. L. Irvine-Fynn, Department of Geography, University of Sheffield, Winter Street, Sheffield S10 2TN, UK.
E-mail: t.irvine-fynn@sheffield.ac.uk

Received 16 June 2003
Accepted 22 October 2003

evolution of a hydraulically efficient subglacial drainage system (e.g. Collins, 1989; Gurnell *et al*., 1992; Richards *et al*., 1996). Researchers have also noted transient 'flushes' of SSC independent of discharge variations in proglacial streams of temperate glaciers. These have been attributed to rainfall events and bank collapse supplying sediment to proglacial streams, but also to subglacial channel migration, in-channel sediment storage and release, and glacier motion (Richards, 1984; Gurnell and Warburton, 1990; Willis *et al*., 1996; Stott and Grove, 2001; Orwin and Smart, 2002).

In Arctic catchments, studies of proglacial stream SSC dynamics have been used to examine the significance of glacial thermal regime on glaciofluvial sediment transfer processes (e.g. Gurnell *et al*., 1994; Hodson and Ferguson, 1999; Hodgkins, 1999). Transient flushes and other SSC variations, including changing lags between SSC and discharge time series, have been identified in Arctic proglacial streams, although their causes remain unknown. To explain such SSC variability, adjustments in sediment source areas related to 'variable ground thaw processes' (Gurnell *et al*., 1994: 333), ground thaw and solifluction processes (Hodson *et al*., 1997, 1998a), and the potential influence of ice-cored moraines (Hodson and Ferguson, 1999) have been implicated. However, most previous studies of SSC in Arctic streams have placed little emphasis on geocryological processes and their interaction with glaciofluvial processes, even through processes of frost weathering, rockfall, thaw-induced debris flows, slumps and collapse, and solifluction in the ice marginal areas may be significant.

Additionally, because permafrost restricts water percolation into the subsurface, runoff in basins underlain by permafrost responds quickly to both snowmelt and rainfall events. Whereas Richards (1984) stressed the importance of a 'rainfall' variable in multivariate statistical models to predict SSC, Willis *et al*. (1996) and Hodgkins (1999) found rainfall was insignificant in explaining SSC variation in proglacial streams in southern Norway and southern Spitsbergen respectively. Where the proglacial sediment source area is small or the gauging station is near the glacier, rainfall will have a much reduced effect on sediment mobilization directly (Willis *et al*., 1996). Further, discharge is highly dependent on rainfall timing and magnitude (Hodson *et al*., 1998b); therefore, enhanced sediment mobilization should accompany accentuated discharge during storm conditions. This suggests that, at high latitudes, geocryological processes may provide spatially and temporally discontinuous sources of sediment to proglacial streams rather than discharge variability alone.

Etzelmüller *et al*. (1996) showed that the prevalence of proglacial ice-cored moraines in Svalbard is directly connected to climatic conditions. In this type of permafrost-influenced proglacial terrain, thermo-erosion during warm periods ensures ice-cored moraines can be important sediment sources. Thermo-erosion is defined here as thaw-induced release of material in the ice-marginal environment. Changes in proglacial surface elevation associated with thermo-erosion and sediment mobilization are considered important for small Arctic valley glaciers (Etzelmüller, 2000). Smaller, high-latitude glacier basins are more affected by slope processes, which are strongly influenced by both the periglacial environment and the ice-proximal fluvial system (Holmlund *et al*., 1996; Etzelmüller *et al*., 2000). Hodson *et al*. (1998a) documented a net increase in sediment source in the ice-proximal zone partially linked to geocryological processes, suggesting that in-channel sediment storage during the ablation season in this region may be small. Further, there is evidence of coupling between glacial and periglacial environments on Bylot Island, Nunavut. Moorman (2003) documented hydrological connectivity between a glacier and the surrounding ice-cored moraines. This highlights the linkage between the glacial and periglacial environments, indicating that thermo-erosional and/or geocryological sediment delivery process may be significant in high-latitude environments. Ground-penetrating radar surveys of proglacial and ice marginal zones on Bylot Island provided evidence of both ice-cored moraines and buried ice still connected to a glacier body (Moorman and Michel, 2000a), conditions that potentially enhance sediment delivery to near-glacier streams through thaw slumps and mass wasting.

In summary, sediment transfer in High Arctic basins may be influenced by storage and release of sediment through glacial, fluvial and periglacial processes. This paper analyses meteorological, proglacial stream discharge, and SSC data from northeast Spitsbergen, Svalbard, and southeast Bylot Island, Nunavut, Canada. Previous research on glacial hydrometeorological time series has employed subjective hydrological or meteorological characterization (e.g. Gurnell *et al*., 1991, 1992, 1994; Hodson *et al*., 1998a,b), hydrograph clustering (e.g. Hannah *et al.*, 1999), and arbitrary division (e.g. Hodgkins, 1996). A more recent technique has been the application of wavelet analysis (e.g. Lafrenière and Sharp, 2003). Here, principal component analysis (PCA), change-point analysis (CPA), and multivariate regression techniques are employed sequentially in an effort to identify the relative importance of thermo-erosion processes in the sediment dynamics of High Arctic basins. The statistical methods introduce an objective technique to subdivide glaciofluvial time series.

METHODS AND FIELD LOCATIONS

Three glacier basins were considered: the adjacent Austre Brøggerbreen and Midre Lovénbreen, northwest Spitsbergen, Svalbard (79 °N, 12 °E) and Glacier B28, southeastern Bylot Island, Nunavut (73 °N, 78 °W) (Figure 1). Austre Brøggerbreen is a north-facing cold-based glacier, dominated by subaerial drainage; the portion of the basin monitored in this study occupies a catchment of 9·8 km^2, of which 71% is permanent ice cover (Hodson *et al.*, 2000). Midre Lovénbreen is a north-facing, polythermal glacier covering 80% of a 7·8 km^2 catchment (Hodson *et al.*, 2000); the temperate ice zone is located in the accumulation area and at the bed in the upper ablation area (Björnsson *et al.*, 1996; Rippin *et al.*, 2003). An area of approximately 5·0 km^2 drained through the stream channel under observation in this study. Annually, Midre Lovénbreen has exhibited subglacial hydrological breakthrough at the cold margin where turbid pressurized water emerges at the snout (Hodson *et al.*, 2000; Rippin *et al.*, 2003). The geology at Austre Brøggerbreen and Midre Lovénbreen is virtually identical, being primarily underlain by phyllite and schists, although sandstones, shale and limestones are present under Austre Brøggerbreen (Hjelle, 1993). Both basins, extending from 50 m to approximately 600 m a.s.l., are underlain by continuous permafrost to depths of approximately 120–400 m (Liestøl, 1977), and both glaciers have exhibited negative mass balances in recent years (Björnsson *et al.*, 1996).

Glacier B28, unofficially named Stagnation Glacier, is a higher elevation, south-facing, polythermal glacier (Moorman and Michel, 2000b) occupying 55% of a 25·5 km^2 catchment on southeastern Bylot Island. Stagnation Glacier is a narrow, retreating valley glacier ranging from 320 to 1050 m a.s.l. in elevation, and is flanked by large ice-cored moraines. The proglacial zone is (partly) ice cored (Moorman and Michel, 2000a). Maximum local permafrost depths are to the order of 400 m (Moorman and Michel, 2000a) and the geology is dominated by Archean igneous and metamorphic rocks (Jackson *et al.*, 1975). The glacier hydrology is dominantly subaerial, with marginal channels and deeply incised supraglacial channels. Qualitative tracer investigations show that moulins near crevasse zones drain en- or sub-glacially to the eastern side of the snout.

Both Midre Lovénbreen and Stagnation Glacier exhibit confined proglacial icings, extending for *c*. 500 m from the glacier snouts. No icing exists at Austre Brøggerbreen because the glacier is cold based.

For all three glaciers, the gauging stations were installed *c*. 500 m from the glacial margin, with comparatively stable upstream channels, that exhibited minimal seasonal migration. Further, armouring, bedrock limitation and icing margins ensured channel stability over the three relatively low-gradient proglacial areas. These factors are assumed to limit in-channel sediment storage and exchange processes upstream from the gauging stations, which are common to more dynamic, multichannel or braided proglacial reaches.

Proglacial discharge (Q) and SSC were measured continuously during the summer at all three sites. Data were collected in 2000 at Austre Brøggerbreen and Midre Lovénbreen and in 2002 at Stagnation Glacier. Measurements of water stage were taken every 1 to 6 min using pressure transducers, from which hourly averages were calculated. Druck pressure sensors were used for the Svalbard basins and a Levellogger probe was used on Bylot Island. Average hourly water stage was converted to Q using stage–discharge curves. Discharge values for these curves were determined using the velocity–area method. Calculated from the standard error, all three Q series exhibit uncertainties between 10 and 20%, similar to errors given by Hodson and Ferguson (1999).

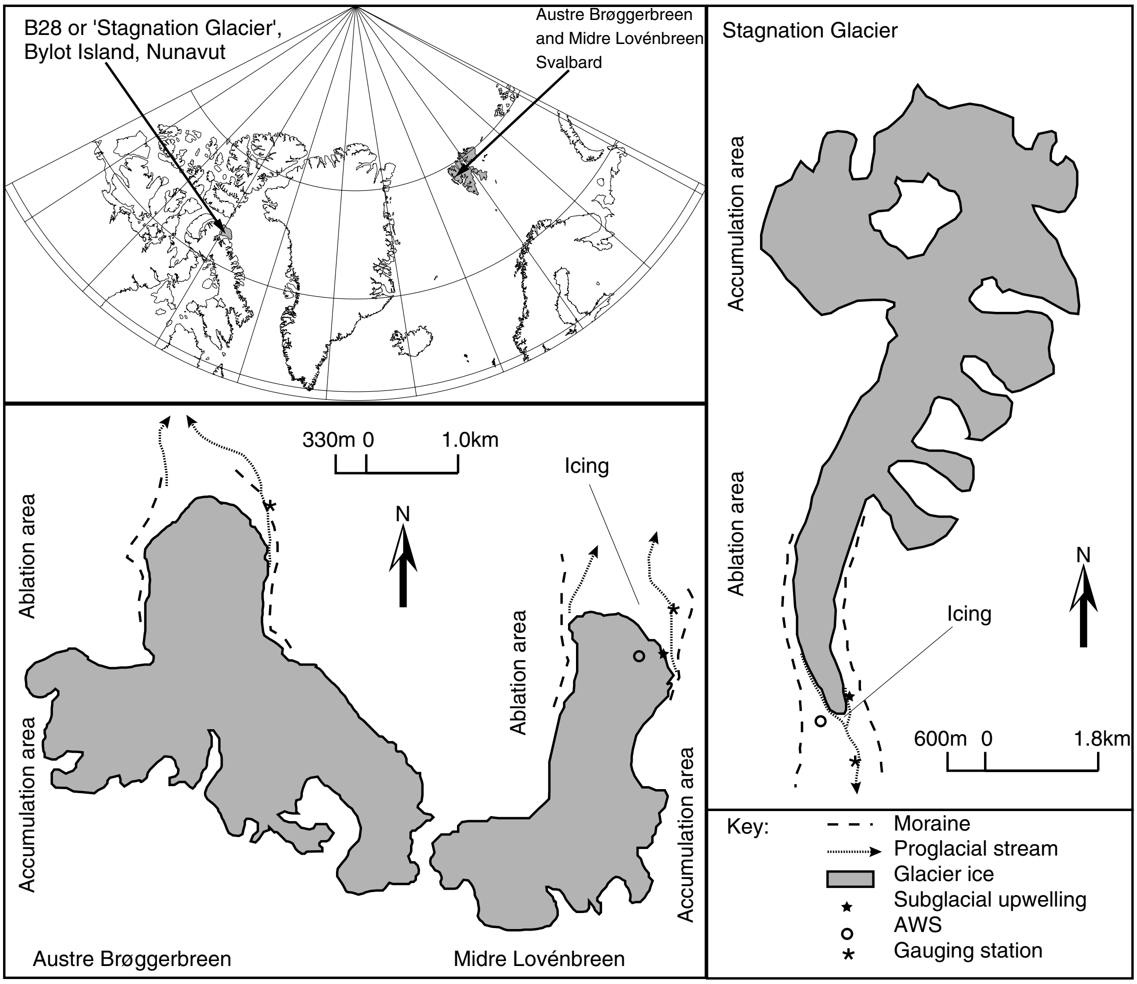

Figure 1. Location map showing study sites and sketch maps of the three glacier basins

SSC was calculated from similarly averaged hourly measurements of turbidity recorded with infrared turbidity sensors. Partech IR-15C probes were used at both Austre Brøggerbreen and Midre Lovénbreen, and a Hydrolab Datasonde turbidity sensor was employed at Stagnation Glacier. Each sensor was calibrated against filtered water samples taken four times per day throughout the monitoring period. The four daily samples corresponded approximately to peak and low flows and two mid-range discharges. The estimates of SSC, using Whatman 0·45 μm filter membranes for the Svalbard basins and 1·2 μm glass-fibre filters at Stagnation Glacier, gave typical errors of <2%. Simple linear rating curves were used to calibrate the turbidity records, although under- and over-prediction is likely at low and high SSC. Derived from standard errors, data suggest SSC error ranges between 32 and 68%.

At Midre Lovénbreen and Stagnation Glacier, Campbell Scientific automatic weather stations (AWSs) recorded air temperature (AT), net radiation and incoming radiation (NRAD and IRAD respectively). At Midre Lovénbreen the AWS was positioned on the glacier snout *c*. 110 m a.s.l., and at Stagnation Glacier the AWS was located *c*. 350 m a.s.l. on a lateral moraine ridge at its western margin. On Svalbard, rainfall was recorded using a standard tipping-bucket, and on Bylot Island the snow and rainfall events were recorded qualitatively. The cold temperatures and summer snow events resulted in poor quantification of rainfall.

Initial analysis of the Svalbard data indicated rainfall was independent from all variables other than discharge; therefore, it was not included in these statistical analyses.

RESULTS

The discharge time series for Midre Lovénbreen and Austre Brøggerbreen showed similar trends, but distinct differences existed in the SSC records (Figure 2). For Austre Brøggerbreen, SSC remained low and relatively constant for the entire season, with the exception of spikes at the start of the monitoring period and a peak of $\sim$1·5 g l^{-1} on Julian day (JD) 199. The likely interpretation is high sediment load from the channel margin during initiation of flow at the start of the season, and following a rainfall event on JD198–JD199. The SSC time series oscillates, indicating a diurnal variation. However, peaks in SSC did not necessarily coincide with peak or rising Q, suggestive of alternative supply mechanisms.

At Midre Lovénbreen, mean SSC was 1·02 g l^{-1}, compared with 0·17 g l^{-1} at Austre Brøggerbreen. A distinct change occurred on JD198, with a switch from low to high SSCs, coinciding with a rainfall event. This increase in turbidity was associated with a breakthrough event at the glacier margin, with subglacial waters effusing initially as an artesian fountain, and later via a more stable channel emerging from the glacier snout. The elevated SSC continued, but gradually declined for the remainder of the ablation season, possibly reflecting the drainage and exhaustion of a subglacial reservoir.

At Stagnation Glacier, Q was considerably greater than at the Svalbard basins, reflecting the larger catchment (Figure 2). Data collection had to be stopped between JD189 and JD192, when logging equipment had to be removed due to a rainstorm-induced flood. SSC averaged 0·25 g l^{-1}, peaking at 3·25 g l^{-1} during the storm runoff, but otherwise the patterns in SSC exhibited diurnal cycles, although not always linked to peak Q (e.g. JD182–189, JD193 and JD194). On JD183, turbid water effused on the glacier surface approximately 1·9 km from the snout. However, this ceased by JD185, and thereafter a turbid outflow emerged at the glacier sole on the eastern side of the snout. The interpretation is that water in a subglacial reservoir initially flowed out of the glacier under high pressure through fractures or weaknesses downglacier from a crevasse zone located approximately 2·0 km from the glacier snout. Englacial and subglacial drainage pathways gradually evolved and water exited the glacier via these pathways thereafter. This breakthrough corresponded with a temporary reduction in the diurnal variability in SSC, although following the rainstorm and snowfall (JD188–JD195), there was a marked increase in this diurnal variability.

For comparison, temperature data for the Svalbard sites and at Stagnation Glacier are shown in Figure 3a and b respectively. Because Austre Brøggerbreen and Midre Lovénbreen are adjacent, meteorological data are assumed to be representative for both basins.

STATISTICAL ANALYSIS

Identification of sub-seasons: PCA

A key limitation to interpreting SSC patterns is the tendency to examine the ablation-season data as a whole (e.g. Hodson and Ferguson, 1999). This gives rise to the 'smothering' of detailed changes in the glacial, fluvial and periglacial processes. To examine the particular (rather than the general) patterns within the data series, we use PCA as an objective method to examine and subdivide the seasonal data set. PCA has been used infrequently in the glaciological literature, yet it is a proven tool in water quality analysis (e.g. Haag and Westrich, 2002; Hodson *et al*., 2002). PCA explores the variance of a data set, where each 'mode' or 'dimension' of variance within a data set is represented by a linear combination, or principal component (PC), of all the variables. The analysis takes n variables and finds combinations of the original variables producing uncorrelated components. The PCs can be seen as measures of underlying 'dimensions' in the data set. For comprehensive reviews, see Jolliffe (1986) and Davis (1986).

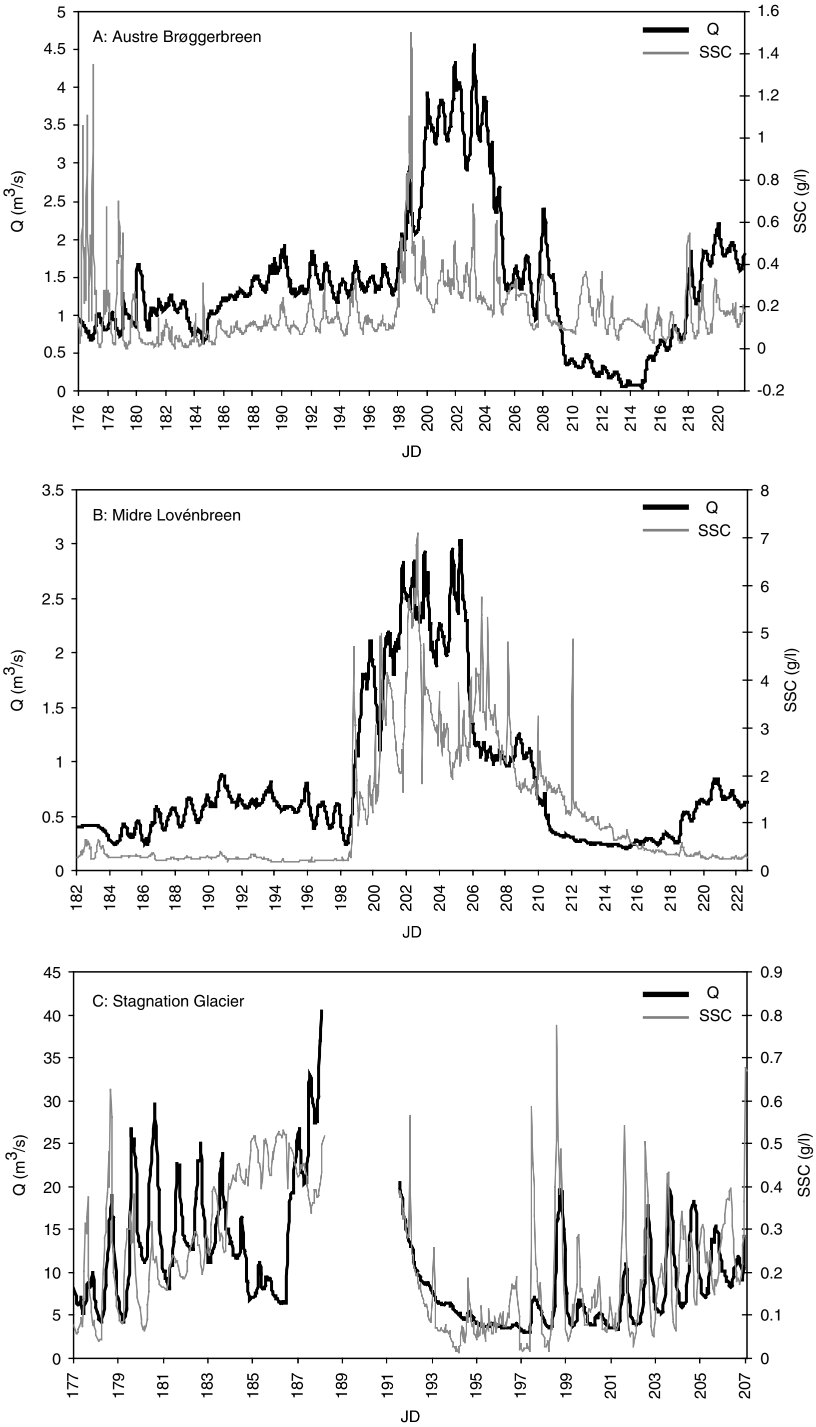

Figure 2. Graphs of raw SSC and *Q* data for Austre Brøggerbreen, Midre Lovénbreen, and Stagnation Glacier. *Q* is the solid dark line, SSC is shown by the grey line. Note, axes scales differ for each glacier

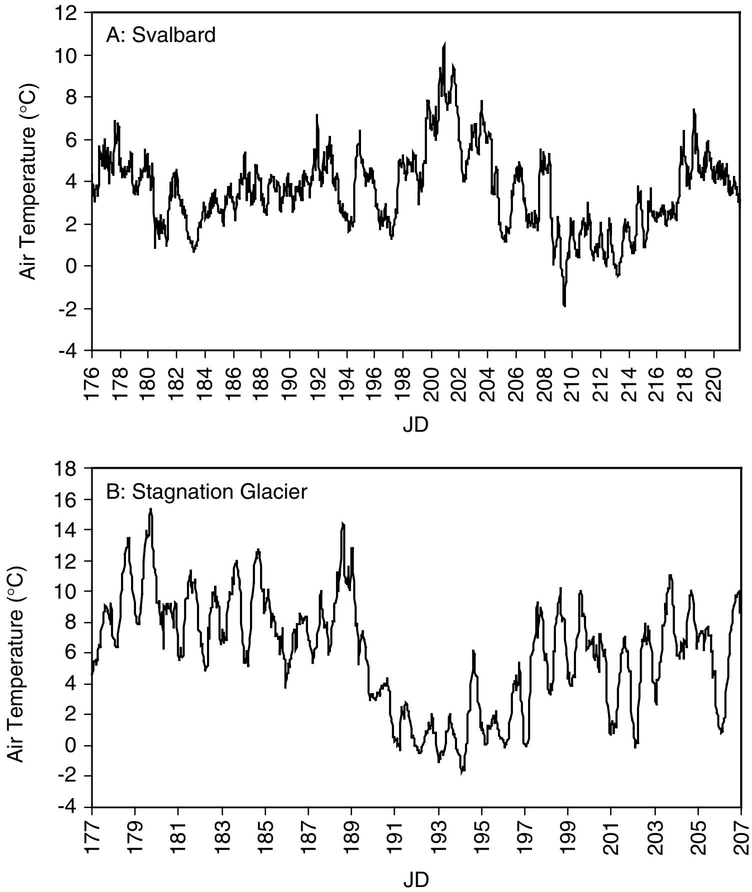

Figure 3. Graphs of raw air temperature (AT) data for Svalbard sites and Stagnation Glacier. Note, the axes scales differ

A complete data set of SSC, Q and AT was used. IRAD and NRAD were used as proxies for synoptic weather patterns and recession of the snowpack (a potential water reservoir) because of their links to cloud cover and albedo. The inclusion of precipitation data was deemed unnecessary (cf. Willis *et al.*, 1996; Hodgkins, 1999). Occasional missing data due to short-term instrument failure (<5 h duration) were filled using a random-walk interpolation filter, accounting for the local data pattern. Less than 3% of any data set is interpolated.

The output from the PCA includes standardized component loadings (Table I). Loadings with opposing sign reflect an inverse relationship. In some cases an inverse association may represent a lagged relationship between two independent variables. PCA on raw data does not account for data sets fluctuating out of phase and, thus, care must be taken with the interpretation of PCA loadings if PCA is the only exploratory statistical tool used.

The first PC (PC1) explains *c*. 50% of the seasonal data variance in all three basins. However, no variable is considered particularly strong for PC1 (all five having positive standardized loadings <0·5). Therefore, we argue that PC1 represents the seasonal trends, inclusive of synoptic weather patterns, hydrological system changes, and variations in glaciofluvial and periglacial processes. PC2 varied for each basin, but generally represented diurnal incoming radiation variability in the Svalbard basins, and a positive relationship between Q and SSC at Stagnation Glacier. PC3 demonstrates the relationship between SSC and AT at Midre Lovénbreen, between SSC and Q at Stagnation Glacier, and the independence of SSC at Austre Brøggerbreen. PC4 and

Table I. Standardized loadings from a five-component PCA analysis. Glacier names are abbreviated, and each component's explanation of variance is shown (%Var). Note in PC3 the apparent relation between SSC and AT at Midre Lovénbreen, between SSC and *Q* at Stagnation Glacier, and the independence of SSC at Austre Brøggerbreen

Glacier	Variable	PC1	PC2	PC3	PC4	PC5
AB	*Q*	0·33	−0·35	−0·41	−0·26	1·45
	SSC	0·37	−0·20	1·05	−0·13	−0·03
	AT	0·38	−0·11	−0·30	0·93	−1·13
	IRAD	0·15	0·60	0·16	0·70	1·04
	NRAD	0·30	0·39	−0·17	−1·12	−0·62
	%Var	45·3	28·8	14·3	7·4	4·1
ML	*Q*	0·32	−0·28	0·02	−0·99	1·68
	SSC	0·29	−0·31	0·78	0·63	−1·17
	AT	0·34	−0·03	−0·85	1·09	−0·22
	IRAD	0·15	0·52	0·48	0·82	1·30
	NRAD	0·28	0·41	−0·06	−1·16	−1·35
	%Var	47·4	32·8	12·9	4·4	2·6
SG	*Q*	0·18	0·50	0·84	0·50	0·08
	SSC	0·19	0·47	−0·84	0·53	0·19
	AT	0·30	0·24	−0·01	−1·25	−0·17
	IRAD	0·34	−0·37	0·03	0·24	4·94
	NRAD	0·34	−0·36	0·01	0·32	−4·90
	%Var	53·5	26·5	10·2	9·5	0·4

PC5 are more difficult to interpret in physical terms and, because they represent <10% of the overall variance, can effectively be considered 'noise'.

The standardized scores derived from PC1 plotted as a time series represent the seasonal and diurnal patterns within the data. Departures from the trend given by PC1 are seen as deviations from the standardized mean, being approximately zero (see Figure 4). The score plot of Stagnation Glacier oscillates to a greater magnitude than the Svalbard basins. We attribute this to the south-facing orientation of the basin, and the associated increased diurnal variability in energy fluxes, resultant *Q* and SSC transport compared with north-facing locations. The score trends for all three basins indicate differing periods, exemplified by the shifts from data trending away from the mean and drifts returning towards the mean. However, visual determination of a fluctuating series trend is highly subjective.

Identification of sub-seasons: CPA

To identify the subseasons objectively from the PC1 score plots, CPA was used. CPA uses a combination of cumulative sum (CUSUM) and bootstrapping techniques. The CUSUM for a time series is calculated as

$$C_t = \sum_{i=1}^{t}(x_i - \overline{x}) \quad (1)$$

where C_t is the cumulative sum value at time t of the variable x_i (here, the standardized PC1 scores) and $\overline{x}$ is the series mean (i.e. of the PC1 scores). Changes in the direction and/or slope of the CUSUM plot are indicative of shifts in the data trend or a change in the local average of the series. To detect these changes objectively, a 'bootstrapping' method was used. Bootstrapping samples the original series without replacement, i.e. re-orders the entire data set by random selection of data points. This random re-ordering of the x_i values allows the generation of bootstrapped CUSUM curves, which are then compared statistically with the original CUSUM plot (Taylor, 2000). Because bootstrapped samples represent random re-orderings

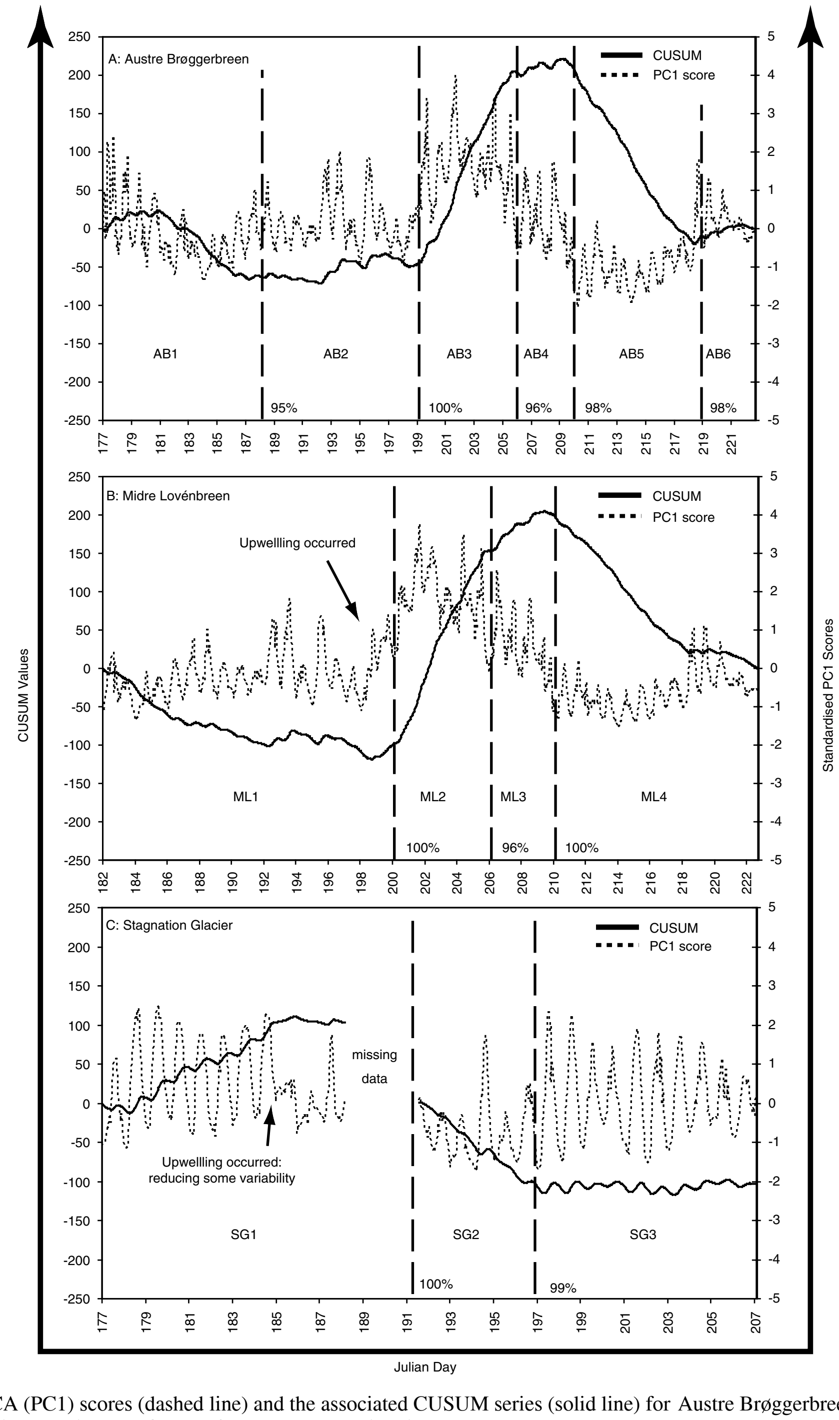

Figure 4. Plots of PCA (PC1) scores (dashed line) and the associated CUSUM series (solid line) for Austre Brøggerbreen, Midre Lovénbreen, and Stagnation Glacier. Confidence for the change points in the data are shown, and subseasons are labelled accordingly

of the data, their CUSUM should mimic the behaviour of the original CUSUM if no change has occurred. Deviations can be perceived as change points, where the bootstrapped CUSUM deviates form the original

Table II. Lag time identified using 'best match' CCFs between SSC and the other variables. Note the lack of coherence or clear trends. Some variables appeared 'in phase' with a lag of $n \pm 12$ h, e.g. where the negative correlation was stronger than a shorter lag-time positive correlation. The lack of clear trends suggests there is poor evidence of a seasonally progressive response between elements of the hydrometeorological system

Sub-period	AB				ML				SG			
	SSC–*Q*	SSC–AT	SSC–IR	SSC–NR	SSC–*Q*	SSC–AT	SSC–IR	SSC–NR	SSC–*Q*	SSC–AT	SSC–IR	SSC–NR
1	−3	0	+17	−5	+2	−3	−16	−16	+3	+16	+13	+12
2	+4	−2	−6	−5	+5	−13	−2	−16	0	+14	+7	+9
3	−9	−6	−6	−6	+12	+13	+7	+7	−3	+2	+12	0
4	+3	0	−4	−2	+14	0	+13	−7				
5	+15	+11	−5	+8								
6	−2	+5	+3	+4								

data pattern. The difference d between the maximum and minimum CUSUM values of each bootstrap is then compared with the original data's d, and from this comparison the confidence of change in the series can be ascertained (Taylor, 2000). For a full account of CPA techniques, refer to Taylor (2000) and Chen and Gupta (2000).

Change-Point Analyzer 2·0 software was used to perform this analysis with a sequence of 1000 bootstraps used to identify breaks within the data. However, one of the limitations of CPA is the problem induced by non-independent errors in the data set. This is common with a strongly autocorrelated data set, such as that containing a diurnal periodicity. Where errors are positively correlated, the analysis may indicate change points incorrectly.

To resolve this issue, a Fourier analysis was used to confirm the presence of a diurnal cycle in the score data sets. For both Svalbard basins, the CPA was conducted using a series of scores for one particular hour. The score values at 00 : 00 (midnight) for each day were used. It is assumed with the cyclic time-series that data points spread 24 h apart are sufficient to identify breaks within the data set as a whole. However, since the data set for Stagnation Glacier was for a shorter duration, and exhibited a break, data were grouped into sets of 24 sequential data points. CPA analysed these daily sets to determine the change points. The change points of the PC1 (seasonal) series are shown on CUSUM plots (Figure 4) with the confidence levels indicated at each change.

Six subperiods or subseasons were identified at Austre Brøggerbreen (AB): AB1 ran from JD177 to JD188, AB2 occurred between JD189 and JD199, during which time Q and SSC exhibited a stable, diurnal trend. AB3 began on JD199, coinciding with a rainfall event, and continued until JD206, during which time Q and SSC were consistently high. A short subseason (AB4) occurred between JD207 and JD210 while Q was falling, and AB5 continued until JD219, during which time snowfall and low temperatures occurred. AB6 represents the culmination of the season. At Midre Lovénbreen, the season is divided into only four subseasons; the first break on JD200 follows the initiation of the subglacial system and rain event (JD198–JD199), ML2 runs from JD200 to JD206 and reflects the period of maximum discharge. ML3 corresponds to AB4, and ML4 concluded the season from JD210 to JD222. At Stagnation Glacier, SG1 corresponds to the initial part of the season, during which time the snowpack receded and subglacial water breakthrough was observed. A break occurs due to the rainstorm, and SG2 (JD191–JD197) was characterized by snowfall and cool temperatures. SG3 (JD197–JD207) exhibited increased diurnal variability in both Q and SSC.

Multivariate subseasonal analysis

Although time-series plots of Q and SSC (Figure 2) suggest diurnal variability and some degree of a positive relationship, the data indicate SSC is not purely a response to variable Q. Recent work on proglacial streams has highlighted the value of multivariate regression models (MRMs) to define the factors causing changes in SSC. This is particularly important when identifying proglacial hydrological processes (Richards, 1984), or subglacial hydrological processes (Willis *et al*., 1996; Hodson and Ferguson, 1999). However, in using MRMs it is necessary to reduce the data's heteroscedasticity, and normalize the dependent variable. The transformation can in practice be restricted to either a logarithmic or square-root function (Vandaele, 1983), so a $\log_{10}$ transformation was applied to the raw Q and SSC data.

MRMs predicting log SSC were developed for each subseason defined by the CPA, using predictor variables relating to discharge including log Q, δQ, ΣQ, $hQ!$, and Q^2. Similar variables have been used in recent analyses (e.g. Richards, 1984; Willis *et al*., 1996; Hodson and Ferguson, 1999; Richards and Moore, 2003). The log Q variable represents instantaneous discharge forcing, and δQ (the rate of change in discharge) accounts for short-term hysteretic behaviour. Q^2 is used to examine a non-linearity, effectively where sediment mobilization is reflected as 10 to the power of squared discharge, and thus where slight changes in Q lead to large changes in SSC. The cumulative discharge since start of subseason (ΣQ) can be used to reflect either exhaustion or an increase of sediment supply during the subperiod. The variable $hQ!$ represents the time since the start of the subseason that discharge at time t was last equalled or exceeded, with $hQ! = 1$ if the preceding hour's value was a greater discharge. This variable was used rather than 'hours since current discharge was equalled or exceeded for 3 h or more (hQ_{ex3}) preferred by Hodson and Ferguson (1999), because the subseasons under consideration are shorter in duration, and values of *hQ*! never dropped to zero (a problem encountered by Hodson and Ferguson (1999)).

All the discharge-related variables were 'best matched' to the log SSC series by identifying the lag/lead over a 24 h period for log *Q* that gave the highest cross-correlation function (CCF). To ascertain the importance of geocryological processes, supplementary MRMs were developed, including AT, IRAD and NRAD as independent variables, each best-matched by cross-correlation to log SSC. Table II shows the lags for each variable as determined by CCFs. There is no coherent pattern in the changing lag times. This contrasts with results from Gurnell *et al*. (1994), who documented decreasing lag times between *Q* and SSC. The changing lags identified here can only be interpreted as changes in dominant hydrological pathways and sediment source processes.

Stepwise regressions were conducted using the lagged variables, and the results are presented in Tables III and IV and Figure 5. The notable finding is that inclusion of AT and radiation variables leads to overall improvements in the models of SSC. The coefficients of determination are only improved by 1% for several subperiods, but up to 25% for others. Only subperiod SG3 shows no change in the R^2 value. This suggests that there were periods when primarily glaciofluvial conditions explained SSC dynamics, and other times when energy fluxes contributed more significantly. This is suggestive of thaw-related sediment supply, rather than discharge, forcing of SSC.

Time-series analysis

The diurnal variations in *Q*, SSC and meteorological data suggest autocorrelation within the data series. This autocorrelation is not completely accounted for by the MRMs. Autocorrelation within an MRM's residuals indicates SSC is not simply forced by hydrological and meteorological conditions, but rather is partly controlled by preceding values. For this reason a Box–Jenkins autoregressive integrated moving average (ARIMA) model (Box and Jenkins, 1976) was fitted to the residuals from the most effective MRMs for each subseason. ARIMA models are expressed as $(pdq)(PDQ)_s$ where d is the level of differencing for the series, and p and q are the order of an autoregressive and moving-average process respectively; (pdq) is the successive data series, and $(PDQ)_s$ refers to a 'seasonal' component, with periodicity s, which in this case is 24 h.

To identify appropriate models, the autocorrelation functions (ACFs) and the partial autocorrelation functions (PACFs) for the residual series were examined (Vandaele, 1983). In all subseasons the residuals

Table III. Hydrology-only models of proglacial SSC. Table shows MRM coefficients of determination and predictor coefficients for each subseason. The most significant predictor for each MRM is in bold. Glacier names are abbreviated, and *k* represents the constant included in the MRMs. Blank entries show variables considered 'non-significant'

Period	R^2	*k*	log *Q*	δQ	Q^2	ΣQ	hQ!
AB1	0·318	−1·530	**−4·913**		0·554	−0·002 34	
AB2	0·390	−1·338			**0·181**	0·000 184	
AB3	0·332	−0·039	**−1·074**				
AB4	0·785	−0·759		−0·298	0.113	**−0·002 90**	
AB5	0·345	−0·859			**−0·253**		−0·000 992
AB6	0·576	−1·375			**0·174**		
ML1	0·647	−0·678	−0.220		**0·248**	−0·000 577	0·001 13
ML2	0·122	0·615				**−0·000 589**	
ML3	0·794	0·703				**−0·004 84**	0·002 73
ML4	0·856	−0·599	0.474			**−0·0108**	−0·000 807
SG1	0·619	−1·468	0.605		0·000 417	**0·000 196**	0·001 38
SG2	0·543	−1·224			**0·002 96**		
SG3	0·567	−2·175	**1·749**		−0·001 02		

Table IV. Energy and hydrology models of proglacial SSC. Table shows MRMs coefficients of determination, and predictor coefficients for each subseason. The most significant predictor for each MRM is in bold. Glacier names are abbreviated, and k represents the constant included in the MRMs. Blank entries show variables considered 'non-significant'. $\uparrow R^2$ represents the improvement in the coefficient of determination from the hydrology-only models

Period	R^2	k	log Q	δQ	Q^2	ΣQ	hQ!	AT	IRAD	NRAD	$\uparrow R^2$
AB1	0·561	−2·523	−2.696		0·395		−0·002 76	**0·165**	0·001 42	0·002 01	0·243
AB2	0·608	−1·492	−3.079	−0·232	0·402	0·0216		0·0249	0·000 206	**0·000 690**	0·218
AB3	0·408	0·324	**−2.135**		0·0281					−0·000 762	0·076
AB4	0·811	−0·823		−0·299	0·0785	**−0·002 44**		0·0241	0·000 225		0·026
AB5	0·387	−0·993			**−0·290**				0·000 900		0·042
AB6	0·726	−0·981	−3.691		0·364				**0·001 87**		0·150
ML1	0·655	−0·658	0.234		**0·243**	−0·000 471	0·0011			−0·000 507	0·008
ML2	0·375	0·462			−0·0229	−0·000 322		**0·0416**	0·000 357		0·253
ML3	0·828	0·618				**−0·004 11**	0·002 30		0·000 478	−0·000 421	0·034
ML4	0·872	0·737	0.663			**−0·009 91**	−0·000 854	−0·0396			0·016
SG1	0·743	−1·644	0.706		0·000 624	**0·000 187**		0·0309	−0·000 342	−0·000 482	0·124
SG2	0·597	−1·150			**0·002 69**			−0·004 60			0·054
SG3	0·567	−2·175	**1·749**		−0·001 72						0·0

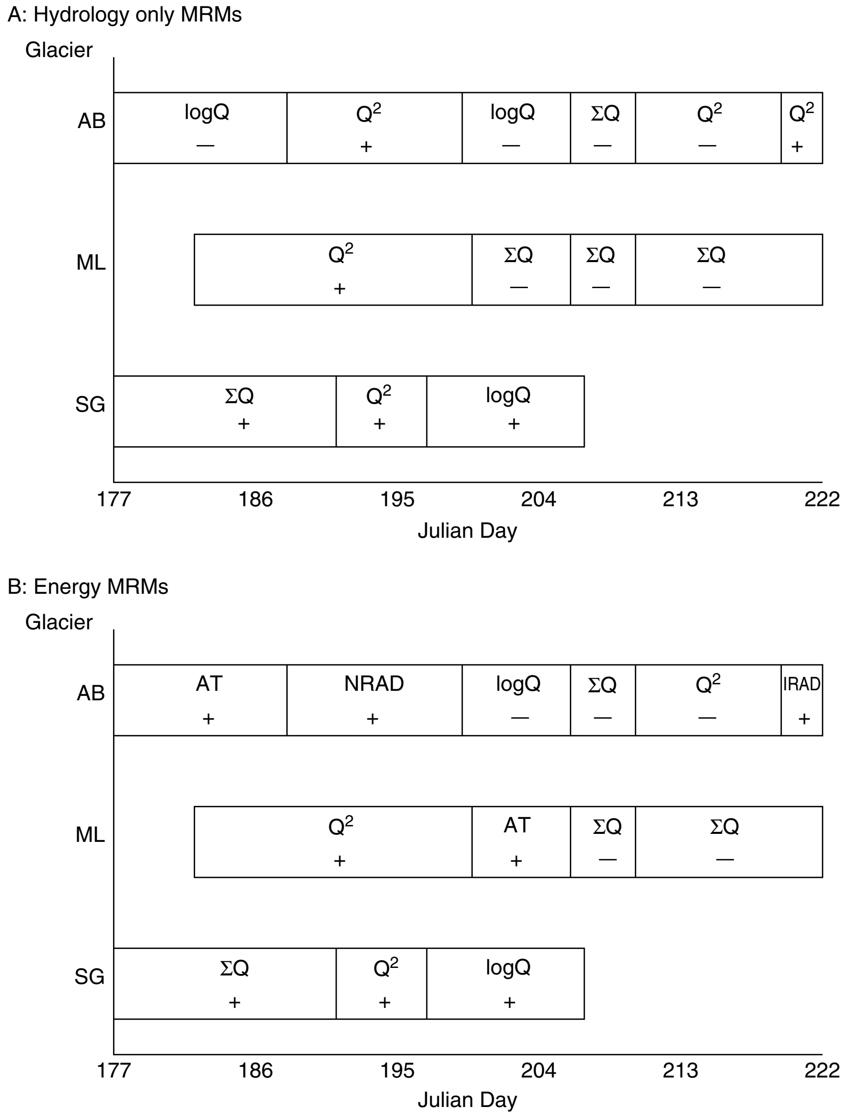

Figure 5. Schematic illustrating the more significant predictors in modelling SSC for the hydrology-only models and the energy models. The sign of the coefficient of determination is indicated

exhibited similar ACF and PACF trends. An exponential decline in significant serial autocorrelation was noted at lags of up to 6 h, with the corresponding PACF only apparent at a lag of 1 h, and no 'seasonal' (diurnal) patterns. This combination of ACF and PACF is indicative of a non-seasonal AR(1) process (Vandaele, 1983). The models were verified by conducting the ARIMA analysis, and parameters were identified with the lowest residual sum of squares (RSS), lowest mean-squared error and T-values significantly different from zero (i.e. $|T| \geq 2$).

The $(100)(000)_{24}$ ARIMA model was clearly defined for all but four of the subseasons for all three data sets. The periods AB5, ML3, SG1 and SG3 were the exceptions; AB5 and ML3 exhibited some autocorrelation remaining with the $(100)(000)_{24}$ model, and improvement was made with an AR(2) model $(200)(000)_{24}$. Both SG1 and SG3 displayed a cyclical pattern in the ACF, indicative of a seasonal trend and some dependence on the previous day's SSC dynamics. The PACF had no notable patterns, and the most effective model reducing all autocorrelation, with $|T| > 2$, was defined as $(200)(110)_{24}$ for SG1 and $(200)(210)_{24}$ for SG3.

These results highlight the importance of autoregressive processes: SSC for all the subseasons in the Arctic basins at any given time was influenced by the preceding hour's value of SSC. Superimposed on this dependence, as part of the ARIMA model, is an element indicative of random changes in sediment supply or source. This result is in keeping with Gurnell *et al.* (1994), who documented a dependence of $\log_{10}$ SSC(t) on $\log_{10}$ SSC($t - 1$) for the hydrological characteristics in the Austre Brøggerbreen basin outlet stream in 1992. The same result was shown by Hodgkins (1999) at Scott Turnerbreen in Svalbard, suggesting short-term supply processes dominate in Arctic basins. The lack of any seasonal component suggests that the MRMs account for diurnal variability fairly well, and the residuals are a stationary series not requiring any differencing procedure.

For the four distinct subseasons (AB5, ML3, SG1 and SG3), the autoregressive process was more attenuated, lasting 2 h in duration. At Stagnation Glacier, the need for seasonal differencing suggests that the MRMs for the two subseasons were less effective in replicating the diurnal variability than the other subseasons considered here. This may be explained by the accentuated diurnal variability seen in the south-facing basin. Further, the seasonal autoregressive component suggests 'memory' in the transport of sediment. During SG1, changes in sediment supply 24 h previously is important for SSC at any given time. In SG3, changes up to 48 h earlier are significant. These results imply either storage or thermo-erosion at channel banks, with material released, irrespective of discharge, on the following day. Interestingly, for SG3, an alternative explanation is changes in subglacial configuration; this is in keeping with Willis *et al.* (1996), who argued that 2 days may reflect the time period of exhaustion or isolation of subglacial sediment sources.

DISCUSSION

Seasonal division

The use of PCA in combination with the subseasons derived from CPA is shown to be an objective method to divide the seasonal data. However, it should be noted that division is only possible on a daily basis, not on an hourly scale. The CPA in this study is a useful alternative to the use of apexes and breakpoints to subdivide a data set manually, as was conducted by Richards and Moore (2003) to infer distinct 'regime shifts' in discharge data. The success of the subdivision following this PCA–CPA technique is exemplified by the different MRMs that were defined for each time period, reflecting changes in the relative importance of fluvial, glaciological and periglacial processes controlling SSC variability.

An interesting avenue for further work is the use of different PCs to subdivide a season on the basis of alternative relationships between variables. PC1 used here is interpreted as defining an overall seasonal trend. Alternatively, PC3, for example, could be used to examine shifts in the negative correlation between SSC and Q and/or AT and the resultant subperiods (see Table I).

MRM interpretation

Seasonal variability in SSC–Q relationships has been reported elsewhere (e.g. Gurnell *et al.*, 1994; Hodgkins, 1996). Here, we present a brief interpretation of the MRMs, demonstrating the potential significance of thaw-related processes, and the nature of subtle changes in the glacial, fluvial and periglacial processes for each subseason.

The failure of any significant contribution to the MRMs by δQ indicates a lack of diurnal hysteresis, although this may be an artefact of the 'best matching' of variables. Previous research in Arctic catchments has noted the lack of coherent hysteresis patterns (e.g. Hodgkins, 1996, 1999), indicating complex SSC response. Therefore, no conclusion relating to diurnal sediment supply variability and hysteretic behaviour due to in-channel storage in any subseason can be offered here.

The improvement of the MRMs by inclusion of temperature and/or radiation data shows that Q and Q-derived variables are insufficient to represent SSC dynamics. However, two sets of interpretations are required: one for the Q-based MRMs and another for the MRMs that include energy variables.

Hydrology-only MRMs.. We consider only the primary or most significant predictor and its coefficient for each MRM in all subperiods (see Table III and Figure 5a) and examine each glacier in turn.

Austre Brøggerbreen:

1. AB1 and AB3. These subseasons are characterized by log Q with negative coefficients indicative of an inverse relationship: sediment mobilization and delivery are not in response to high Q, rather high SSC is seen at times of low water stage. We interpret this as a dilution effect, indicating a limit on the sediment supply source; thus, despite increasing flows, SSC does not increase. Snow cover and the influence of permafrost at the ice margins in the early ablation season (AB1), and high ice melt rates during AB3, could explain the limits on sediment concentration during these times.
2. AB2 and AB6. Q^2 acts as the most effective predictor. Positive coefficients suggest that small increases in Q lead to larger non-linear increases in SSC. This, we argue, is related to stream flow and hydraulic radius. The conjecture is that entrainment potential is related to turbulence and viscous dissipation both at the bed and at the immature, unconsolidated banks. A slight increase in Q leads to an increase in hydraulic radius, allowing sediment at the banks to be mobilized, coupled with likely increases in turbulence to enhance entrainment. We suggest that this demonstrates the sensitivity of permafrost-influenced stream margins, where sediment destabilization may occur in response to thermo-erosion initiated by contact with meltwater streams. This was observed to occur during periods that follow snowline recession, and the removal of the insulating layer, enabling thaw-related processes to operate unabated at the unconsolidated regions of the up-glacier stream margin. Snowpack recession can aid initiation of ice-marginal mass movements over a progressively larger area (Hodson *et al.*, 1998a). Further, both periods are of relatively steady discharge, suggesting thermo-erosion, since channel migration was minimal. Although this result may represent in-channel storage/release, the lack of consistent hysteretic behaviour suggests that thaw processes may be more significant.
3. AB4. A negative coefficient for ΣQ is apparent for this subseason. The negative coefficient indicates subseasonal exhaustion of subaerial sediment source areas as the channel stabilizes at the ice margin. The high discharges during AB3, while mobilizing and transporting significant quantities of sediment, may have effectively limited the sediment source available at lower discharges, ensuring apparent exhaustion subsequently.
4. AB5. A negative coefficient for Q^2 shows that small increases in Q resulted in large decreases in SSC. Q was very low during this period, owing to a snowfall event on JD210, whereas SSC remained fairly high. The best match lag between SSC and Q for this subperiod is $+15$ h, with a negative CCF. However, there was no significant positive correlation over a ± 24 h lag time. This indicates that the inverse relation between SSC and Q is not a product of the best-match procedure. Therefore, to explain this pattern, we suggest that initial snowmelt may have mobilized fine sediments even at low discharges, thus increasing possible in-channel storage at the ice margin, or the source area at the channel margins. Thereafter, although Q was low, any increase following snowmelt diluted the SSC, causing the apparent reduction in sediment transport. This implies that a fairly static, constant sediment source exists during this time.

Midre Lovénbreen:

1. ML1. Q^2 with a positive coefficient reflects the development of the channel and erosion of the stream banks early in the ablation season as the headwater source increases in elevation, and discharge variability remains relatively stable (see AB2 above).
2. ML2, ML3 and ML4. All these subseasons exhibit sediment supply exhaustion indicated by the negative coefficient for ΣQ. We interpret this to reflect the progressive exhaustion of a subglacial reservoir. ML2

begins shortly after the upwelling (JD198), indicating that, following the establishment of a subglacial route, sediment source area starts to be exhausted. The pattern of exhaustion continues for the remainder of the season throughout ML3 and ML4. Exhaustion of a subglacial reservoir would occur as a route stabilizes, or remains stable. It is possible that evolution towards a more efficient drainage system leads to exhaustion; however, more evidence would be required to assert this. Additionally, as seen at Austre Brøggerbreen (AB4), any ice marginal sediment inputs are probably lessened later in the ablation season.

Stagnation Glacier:

1. SG1. ΣQ with a positive coefficient indicates a subseasonal increase in sediment supply. We interpret this to reflect the enlargement of drainage area following the retreat of the snowline and the associated augmentation of the sediment source area early in the ablation season. This subaerial development of drainage is coupled with the emergence of subglacial water (JD183) continuing until the rain storm that divides SG1 and SG2.
2. SG2. During this period of snowfall and lower temperatures, Q^2 with a positive coefficient suggests SSC dynamics are in response to thermo-erosion as the streams re-establish themselves following the demise of the temporary summer snow cover (see AB2). Additionally, for the subglacial system, this may indicate that higher flows periodically access or erode sediments proximal to or at the channel edges and/or cause migration of subglacial channels.
3. SG3. The positive coefficient for log Q suggests that SSC is directly forced by Q. Sediment mobilization is a function of the volume and velocity of discharge passing through the hydrological system. This implies that fluvial processes dominate SSC dynamism.

In summary, the interpretation of predictor variables is dependent on both the sign of the coefficient and, more importantly, on the context of the physical setting. For example, ΣQ, as a term reflective of sediment supply exhaustion or increase, has different interpretations for cold-based Austre Brøggerbreen and the subglacial reservoir of Midre Lovénbreen. However, several key points can be surmised. The cold-based Austre Brøggerbreen shows that SSC appears highly sensitive to geocryological and ice marginal processes; ground frost may limit sediment supply, but thermo-erosion and bank destabilization enhance SSC. At the polythermal Midre Lovénbreen, the SSC dynamics are dominated by the exhaustion of the subglacial reservoir, although the initial part of the season shows the possible influence of periglacial processes.

For Stagnation Glacier, extension of the drainage area is seen early in the season; however, following the rain event, exhaustion of the subglacial reservoir is not observed. Hodson and Ferguson (1999) found, for the polythermal Erdmannbreen, that exhaustion was not detected. Three explanations were provided: (i) effective ice-marginal sediment delivery; (ii) processes controlling sediment delivery in the immediate proglacial environment, in particular for ablation of icings enhancing sediment transfer; or (iii) poorly understood changes in the subglacial drainage structure (Hodson and Ferguson, 1999). The high-intensity rainfall event at Stagnation Glacier may have 'forced' the development of a hydraulically efficient route by effectively scouring the subglacial sediment source area. Similar responses to unusual flood events have been documented for Bas Glacier d'Arolla by Warburton and Fenn (1994). An alternative explanation is that the subglacial system is less spatially extensive at Stagnation Glacier compared with Midre Lovénbreen, and ice-marginal and icing degradation sediment supply outweigh the subglacial signal. Either through the development of an efficient subglacial system, or as a result of the extra-glacial processes, the latter two subseasons would be characterized by SSC dynamics directly or indirectly forced by changes in Q. This contention is also suggested by the results of the ARIMA analysis.

Energy MRMs. In considering the MRMs including energy terms (Table IV and Figure 5b), four of the subperiods show a dominance of AT, IRAD or NRAD in prediction of SSC, which indicates that thaw or thermo-erosional processes may be important. This links SSC directly to meteorological variables. Positive coefficients for energy predictor variables are apparent for AB1, AB2, AB6 and ML2; high SSC is related to high air temperatures or radiative energy. High temperatures and radiation receipt would enhance thaw in frozen sediments in the ice-marginal and proglacial environment, or destabilize ice-cored slopes, thus contributing to sediment inputs to streams. The positive link between SSC and AT during ML2, when subglacial waters were emerging from the glacier snout, suggests that meltwater temperatures may be significant. Thermo-erosion could possibly occur in the subglacial environment; however, no evidence is available to confirm this assertion. Positive coefficients are apparent for IRAD in all cases, suggestive of links between SSC and solar radiation. Despite the changes in coefficients, the MRMs incorporating the energy variables still allude to the same fluvial, glacial or periglacial processes implied by the discharge-based MRMs. The sign of the primary coefficient of determination in the Q-based MRMs remains the same for all the energy MRMs. Some negative relationships are hard to explain, although the best-matching procedure may put variables out of phase.

Thermo-erosion, thaw flows or slumps, and solifluction from ice-cored moraines at the ice margin would be methods of sediment supply directly linked to variability in radiative energy. Although these processes are unlikely to dominate, they may be significant in explaining short-term SSC variability or have contributions to the SSC dynamics during periods of specific hydrometeorological conditions.

In summary, we have presented a broad interpretation of the MRMs. Subseasons demonstrate shifts in the dominant factor dictating SSC. In particular, 'switches' between fluvial, glacial and periglacial processes are implied by the differing MRM variables in each subseason. During these specific hydrological subperiods, sediment release, source exhaustion and thermo-erosional processes at the ice margins may be more significant than has previously been documented in SSC analyses.

ARIMA models

In the analyses presented, the ARIMA model type indicating autoregressive patterns is apparent for all subseasons, indicating sediment 'flushes' were not highly transient, but rather had durations of several hours, generating real autocorrelation in the residuals of MRMs. The ARIMA analysis showed the dependency between SSC at time t and $t - 1$ for 10 of the subseasons, showing that once sediment is mobilized it takes over an hour to settle or be transported. For AB5 and ML3, the AR(2) model indicates that, for the period of relatively stable discharge, a short-term sediment source took longer to be exhausted. For Stagnation Glacier, the appearance of a seasonal autoregressive component suggests that, for SG1 and SG3, where discharge was both higher and more oscillatory than in the Svalbard basins, sediment mobilized on high discharges on one day were deposited at lower discharges, then remobilized on higher discharges the following day. However, the inability of the MRMs to replicate the diurnal variability at Stagnation Glacier is suggestive that processes unaccounted for may be significant in sediment delivery. For this reason, in-channel storage may not be the critical delivery process; rather, it may be cyclic geocryological delivery. The conclusion here is that an element of 'memory' in SSC may occur in larger Arctic basins dominated by subaerial drainage routes.

The stochastic nature of supply processes is indicated by the remaining random *white noise*. The success of an AR(1) model has been argued to indicate that Arctic proglacial streams exhibit short-term sediment availability (e.g. Hodgkins, 1999). Field observation revealed several potential sources of these inputs and causes for short-term elevated sediment availability. Geocryological processes were seen at all three basins. Austre Brøggerbreen, exhibited debris flow lobes superimposed on snowbanks above the stream channel at the glacier margin. At Midre Lovénbreen and Stagnation Glacier, collapse and recession of the icing at the stream margin was observed. Other stochastic inputs from the undercutting of the glacier margin, rockfalls from supraglacial debris and thaw-induced slumping of material from ice-cored moraines were observed at all three field sites.

Implications

In combining MRMs and ARIMA results several points have emerged. The autoregressive models imply that, throughout the ablation season in these Arctic basins, SSC at any given time relates to previous values, with a stochastic component. We contend that, whilst this is true, particularly in light of the ARIMA results, there are greater subtleties underlying this characteristic pattern of drainage.

Austre Brøggerbreen, the cold glacier, shows a dominance of channel marginal and fluvial processes in dictating the patterns of SSC. This can be attributed to the solely subaerial drainage system, where periglacial processes may be a factor partially controlling the sediment supply source. At Midre Lovénbreen it is primarily the subglacial exhaustion that dictates the seasonal dynamics of the sediment carried by the stream channel. And at Stagnation Glacier, it appears that a combination of glacial, geocryological and fluvial processes dominate. However, meteorological conditions may be in part the forcing factor on SSC dynamics, particularly snowfall and rainstorm events, in addition to thermo-erosion, and it is harder to make comparisons between differing glacier basins.

Incorporation of the energy variables serves to improve the models of SSC, implying the importance of thaw or thermo-erosion process contribution. Despite the changes in the models, the processes identified in Q-based MRMs are still apparent in the energy MRMs.

CONCLUSIONS

The mainstay of this paper is the introduction of a statistical method of dividing hydrological data that does not depend on hydro-meteorological characterization or clustering of 'like' hydrographs (e.g. Gurnell *et al*., 1991, 1994; Hannah *et al*., 1999). Further, this paper focuses on inferences regarding thaw-related processes, rather than providing a comprehensive glacial and fluvial hydrological interpretation. The following conclusions can be surmised.

1. The combination of PCA and CPA is a powerful, objective method to subdivide a seasonal data set successfully. The data series can be split into smaller subdivisions with contrasting environmental conditions. Use of PCs other than PC1 would enable seasonal division on the basis of differing relationships between variables.
2. Subseasonal multiple regression analysis of the data demonstrates complexity in hydrological changes. Polythermal glaciers show the importance of subglacial reservoir drainage, potentially obscuring changes in other processes contributing to SSC dynamics. The cold-based glacier indicates a simple hydrology more liable to respond to changing environmental conditions. Changes or 'switches' between fluvial, glacial and periglacial or geocryological processes contributing to SSC dynamics are exemplified in these analyses.
3. In all cases examined, the inclusion of AT, IRAD and NRAD increased the MRM's coefficients of determination by up to 25%. These energy variables, considered independent from Q, would be controls on geocryological slope processes. The multivariate analysis presented here demonstrates that proglacial stream SSC dynamics may be influenced appreciably by thermo-erosional slope processes at the ice margin. Under specific climatic conditions, large quantities of sediment may be released and transported from the periglacial environment.
4. ARIMA models demonstrated the importance of autoregressive components showing SSC dependency on the sediment transport during the preceding hour. This, therefore, supports notions of short-term, spatially and temporally discontinuous sediment supply processes.

Distinct differences in processes do exist between glacier basins and over the course of an ablation season. The importance of geocryological influences (e.g. thaw slumps, solifluction, frost weathering and icing denudation) operating at high latitudes should not be ignored. These results show that, at least for small Arctic valley glaciers, sediment supply is effectively linked to periglacial slope and ice-proximal processes. The temporal variability of climate is a significant control on sediment yield, and in high latitudes, geocryological processes may operate over long time scales. Thus, the possible significance of thaw-related processes and their effects on sediment transport from glacier margins should be accounted for when using sediment yields or sedimentary records in climate and environmental reconstruction.

ACKNOWLEDGEMENTS

The following sources of support for this research are acknowledged: NERC (AJH in receipt of grant GR8/04339), Department of Indian Affairs and Northern Development (NSTP), CFI, Canadian Memorial Foundation, NSERC, University of Cambridge (Worts Travelling Scholars Fund, Scandinavian Studies Fund, Department of Geography, Fitzwilliam College), Alberta Ingenuity Fund, Polar Continental Shelf Project, Norsk Polarinstitutt, Kings Bay Kull Compani, and Parks Canada. Also, the communities of Ny Ålesund, Spitsbergen, and Pond Inlet, Nunavut. And thanks are owed to Nick Cox, Adrian Hayes, Phil Hughes, Brenda Mottle, and Peter Wynn. Two anonymous reviewers are thanked for comments that improved this manuscript.

REFERENCES

Björnsson H, Gjessing Y, Hamran S-E, Hagen J, Liestøl O, Pálsson F, Erlingsson B. 1996. The thermal regime of sub-polar glaciers mapped by multi-frequency radio-echo sounding. *Journal of Glaciology* **42**: 23–32.

Box GPE, Jenkins GM. 1976. *Time Series Analysis, Forecasting and Control*, revised edition. Holden-Day: San Fransisco.

Brown GH. 2002. Glacier meltwater hydrochemistry. *Applied Geochemistry* **17**: 855–883.

Chen J, Gupta AK. 2000. *Parametric Statistical Change Point Analysis*. Birkäuser: Boston; 192.

Collins DN. 1989. Seasonal development of subglacial drainage and suspended sediment delivery to meltwaters beneath an alpine glacier. *Annals of Glaciology* **13**: 45–50.

Davis J. 1986. *Statistics and Data Analysis in Geology*, second edition. Wiley: New York.

Etzelmüller B. 2000. Quantification of thermo-erosion in proglacial areas—examples from Svalbard. *Zeitschrift für Geomorphologie, Neue Folge* **44**: 343–361.

Etzelmüller B, Hagen JO, Vatne G, Ødegård RS, Sollid JL. 1996. Glacier debris accumulation and sediment deformation influenced by permafrost: examples from Svalbard. *Annals of Glaciology* **22**: 53–62.

Etzelmüller B, Ødegård RS, Vatne G, Mysterud RS, Tonning T, Sollid JL. 2000. Glacial characteristics and sediment transfer system of Longyearbreen and Larsbreen, western Spitsbergen. *Norsk Geografiska Tidsskrift* **54**: 157–168.

Gurnell AM, Warburton J. 1990. The significance of suspended sediment pulses for estimating suspended sediment load and identifying suspended sediment sources in alpine glacier basins. In *Hydrology in Mountainous Regions. I—Hydrological Measurements: The Water Cycle*, Lang H, Musy A (eds). IAHS Publication No. 193. IAHS Press: Wallingford; 463–470.

Gurnell AM, Clark MJ, Tranter M, Brown GH, Hill CT. 1991. Alpine glacier hydrology inferred from a proglacial river monitoring programme. In *Proceedings of the British Hydrological Society, Third National Hydrological Symposium* 9–16 September, Southampton, UK; 5·9–5·16–.

Gurnell AM, Clark MJ, Hill CT. 1992. Analysis and interpretation of patterns within and between hydroclimatological time series in an alpine glacier basin. *Earth Surface Processes and Landforms* **17**: 821–839.

Gurnell AM, Hodson AJ, Clark MJ, Bogen J, Hagen JO, Tranter M. 1994. Water and sediment discharge from glacier basins: and arctic and alpine comparison. In *Variability in Stream Erosion and Sediment Transport*, Olive LJ, Loughran RJ, Kesby JA (eds). IAHS Publication No. 224. IAHS Press: Wallingford; 325–334.

Haag I, Westrich B. 2002. Processes governing river water quality identified by principal component analysis. *Hydrological Processes* **16**: 3113–3130.

Hannah DM, Gurnell AM, McGregor GR. 1999. A methodology for investigation of the seasonal evolution in proglacial hydrograph form. *Hydrological Processes* **13**: 2603–2621.

Hjelle A. 1993. *Geology of Svalbard*. Norsk Polarinstitutt Handbook 7; 163.

Hodgkins R. 1996. Seasonal trend in suspended sediment transport from an Arctic glacier, and implications for drainage system structure. *Annals of Glaciology* **22**: 142–151.

Hodgkins R. 1997. Glacier hydrology in Svalbard, Norwegian High Arctic. *Quaternary Science Reviews* **16**: 957–973.

Hodgkins R. 1999. Controls on suspended-sediment transfer at a High-Arctic glacier, determined from statistical modelling. *Earth Surface Processes and Landforms* **24**: 1–21.

Hodgkins R, Tranter M, Dowdeswell JA. 1997. Solute provenance, transport and denudation in a High Arctic glacierized catchment. *Hydrological Processes* **11**: 1813–1832.

Hodson AJ, Ferguson RI. 1999. Fluvial suspended sediment transport from cold and warm-based glaciers in Svalbard. *Earth Surface Processes and Landforms* **24**: 957–974.

Hodson AJ, Gurnell AM, Tranter M, Bogen J, Hagen JO, Clark MJ. 1998a. Suspended sediment yield and transfer processes in a small High-Arctic glacier basin, Svalbard. *Hydrological Processes* **12**: 73–86.

Hodson AJ, Gurnell AM, Washington R, Tranter M, Clark MJ, Hagen JO. 1998b. Meteorological and runoff time-series characteristics in a small High-Arctic glaciated basin, Svalbard. *Hydrological Processes* **12**: 509–526.

Hodson AJ, Tranter M, Dowdeswell JA, Gurnell AM, Hagen JO. 1997. Glacier thermal regime and suspended-sediment yield: a comparison of two High-Arctic glaciers. *Annals of Glaciology* **24**: 32–37.
Hodson AJ, Tranter M, Vatne G. 2000. Contemporary rates of chemical denudation and atmospheric CO_2 sequestration in glacier basins: an arctic perspective. *Earth Surface Processes and Landforms* **25**: 1447–1471.
Hodson AJ, Tranter M, Gurnell AM, Clark MJ, Hagen JO. 2002. The hydrochemistry of Bayelva, a High Arctic proglacial stream in Svalbard. *Journal of Hydrology* **257**: 91–114.
Holmlund P, Burman H, Rost T. 1996. Sediment-mass exchange between turbid meltwater streams and proglacial deposits of Storglaciären, northern Sweden. *Annals of Galciology* **22**: 63–67.
Jackson GD, Davidson A, Morgan WC. 1975. Geology of the Pond Inlet map area, Baffin Island, District of Franklin. *GSC Paper* **74–25**: 1–33.
Jolliffe IT. 1986. *Principal Component Analysis*. Springer-Verlag: New York.
Lafrenière M, Sharp M. 2003. Wavelet analysis of inter-annual variability in the runoff regimes of glacial and nival stream catchments, Bow Lake, Alberta. *Hydrological Processes* **17**: 1093–1118.
Liestøl O. 1977. *Pingos, Springs and Permafrost in Spitsbergen*. Norsk Polarinstitutt Årbok 1975; 7–29.
Moorman BJ. 2003. Glacier–permafrost hydrology interactions, Bylot Island, Canada. In *Proceedings of the 8th International Conference on Permafrost*, Zurich, Switzerland, 21–25 July, Phillips M, Springman SM, Arenson LU (eds). AA Balkema: Lisse; 783–788.
Moorman BJ, Michel FA. 2000a. The burial of ice in the proglacial environment on Bylot Island, arctic Canada. *Permafrost and Periglacial Processes* **11**: 161–175.
Moorman BJ, Michel FA. 2000b. Glacial hydrological system characterization using ground penetrating radar. *Hydrological Processes* **14**: 2645–2667.
Orwin JF, Smart CC. 2002. Short-term spatial and temporal patterns of proglacial suspended sediment transfer, Small River glacier, British Columbia. In *Geological Association of Canada and Mineralogical Association of Canada, Joint Annual Meeting*, Saskatoon, Saskatchewan, 27–29 May; abstract.
Richards G, Moore RD. 2003. Suspended sediment dynamics in a steep, glacier fed mountain stream, Place Creek, Canada. *Hydrological Processes* **17**: 1733–1753.
Richards KS. 1984. Some observations on suspended sediment dynamics in Storbregrova, Jotunheimen. *Earth Surface Processes and Landforms* **9**: 101–112.
Richards KS, Sharp M, Arnold N, Gurnell A, Clark M, Tranter M, Nienow P, Brown G, Willis I, Lawson W. 1996. An integrated approach to modelling hydrology and water quality in glacierized catchments. *Hydrological Processes* **10**: 479–508.
Rippin D, Willis I, Arnold N, Hodson A, Moore J, Kohler J, Björnsson H. 2003. Changes in geometry and subglacial drainage of Midre Lovénbreen, Svalbard, determined from digital elevation models. *Earth Surface Processes and Landforms* **28**: 273–298.
Schiefer E, Slaymaker O, Klinkenberg B. 2001. Physiographically controlled allometry of specific yield in the Canadian Cordillera: a lake sediment-based approach. *Geografiska Annaler, Series A: Physical Geography* **83**: 55–65.
Stott TA, Grove JR. 2001. Short-term discharge and suspended sediment fluctuations in the proglacial Skeldal River, north-east Greenland. *Hydrological Processes* **15**: 407–423.
Syvitski JPM. 2002. Sediment discharge variability in arctic rivers: implications for a warmer future. *Polar Research* **21**: 323–330.
Taylor WA. 2000. *Change-point analysis: a powerful new tool for detecting changes*. http://www.variation.com/cpa/tech/pattern.html [February 2003].
Vandaele W. 1983. *Applied Time Series and Box–Jenkins Models*. Academic Press: New York.
Wadham JL, Hodson AJ, Tranter M, Dowdeswell JA. 1998. The hydrochemistry of meltwaters draining a polythermal-based, High Arctic glacier, south Svalbard: I: the ablation season. *Hydrological Processes* **12**: 1825–1849.
Wadham JL, Cooper RJ, Tranter M, Hodgkins R. 2001. Enhancement of glacial solute fluxes in the proglacial zone of a polythermal glacier. *Journal of Glaciology* **47**: 378–386.
Warburton J, Fenn CR. 1994. Unusual flood events from an alpine glacier: observations and deductions on generating mechanisms. *Journal of Glaciology* **40**: 176–186.
Willis IC, Richards KS, Sharp MJ. 1996. Links between proglacial stream suspended sediment dynamics, glacier hydrology and glacier motion at Midtdalsbreen, Norway. *Hydrological Processes* **10**: 629–648.

